

Supplementary Information

Effect of composition and freeze-thaw on the network structure, porosity and mechanical properties of Polyvinyl-alcohol/Chitosan hydrogels

Fernando Soto-Bustamante^{1,2}, Gavino Bassu^{1,2}, Emiliano Fratini^{1,2} and Marco Laurati^{1,2*}

¹ Dipartimento di Chimica, Università di Firenze, 50019 Sesto Fiorentino, Italy

² Consorzio per lo Sviluppo dei Sistemi a Grande Interfase (CSGI), c/o Università di Firenze, 50019 Sesto Fiorentino, Italy

*Correspondence: marco.laurati@unifi.it

We report additional experimental data and extracted parameters that complement those presented in the main article. Section 1 reports EWC values for gels obtained with FT cycles F12/T12 and F18/T6, and exemplary kinetic curves used to determine EWC, for gels obtained with F6T18. Section 2 presents additional SAXS measurements and the corresponding parameters obtained from modeling for: i) samples containing high Mw Chitosan and obtained through Freeze-Thaw cycles F6/T18 and F18/T6, ii) samples containing medium Mw Chitosan and obtained through Freeze-Thaw cycles F6/T18, F12/T12 and F18/T6. Section 3 reports a comparison of SEM images, confocal stacks and porosity renderings of samples containing high Mw Chitosan and obtained through Freeze-Thaw cycles F6/T18, F12/T12 and F18/T6. Section 4 presents i) plots of the parameters characterizing the 2D porosity of samples containing high Mw Chitosan. ii) plots of the distributions of pore volumes and sphericity of samples containing high Mw Chitosan and obtained through Freeze-Thaw cycles F12/T12 and F18/T6. Section 5 reports linear viscoelastic moduli obtained from oscillatory rheology of samples containing high Mw Chitosan and obtained through Freeze-Thaw cycles F12/T12 and F18/T6

1. Swelling behavior

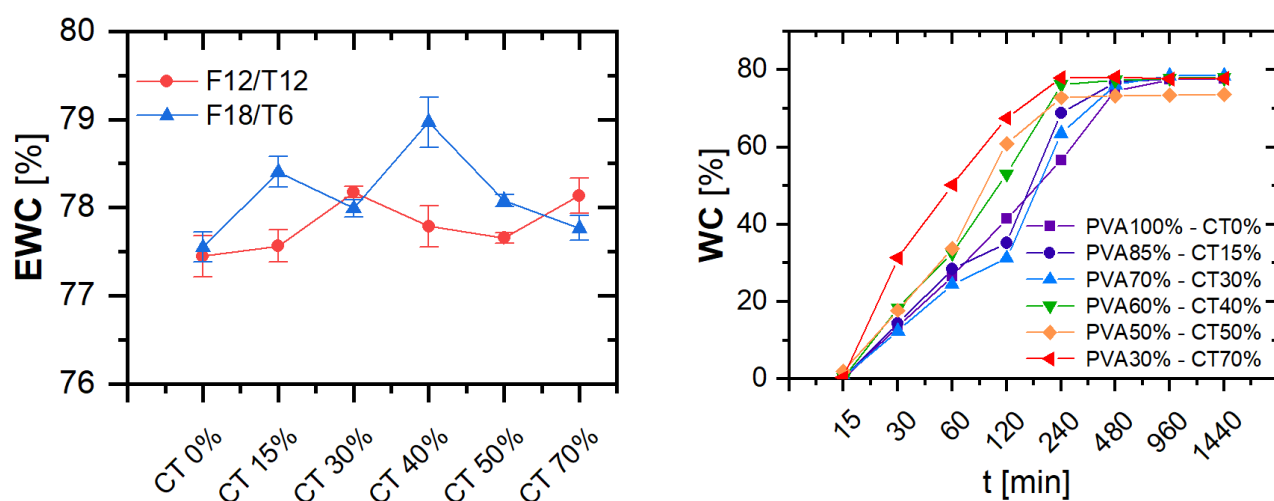


Figure S1. Left: Equilibrium water content (EWC) for the freeze-thawing cycles F12/T12 and F18/T6 as a function of Chitosan content. To drain excess water unconnected into the gel structure, all hydrogels were centrifuged at 1000 rpm for 10 minutes. Right: Exemplary kinetic adsorption curves used to determine EWC, for gels obtained with F6T18.

2. Nanoscale structure, SAXS parameters and plots

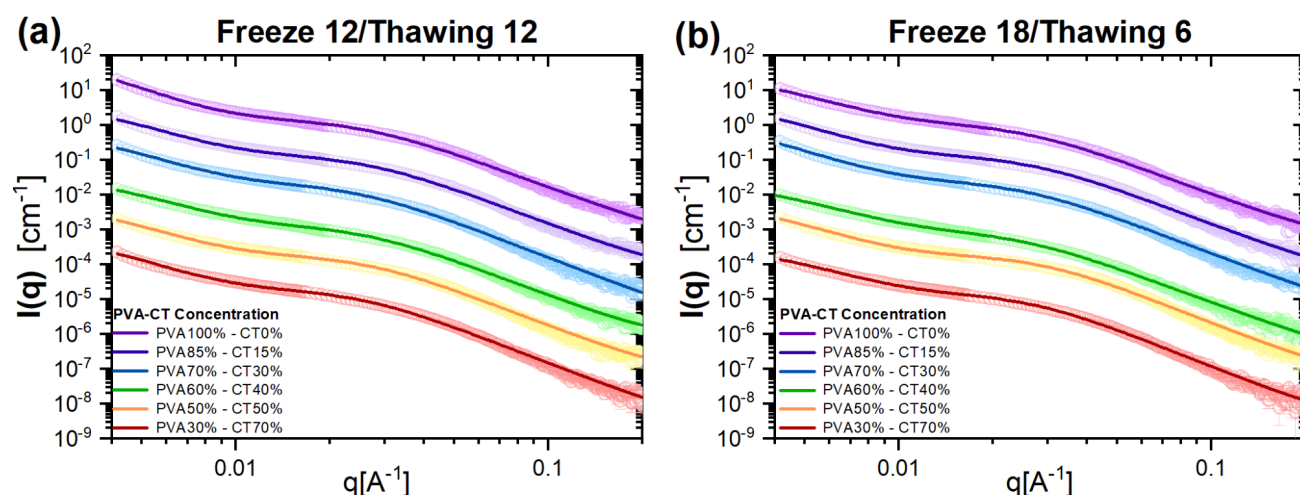


Figure S2. SAXS intensity curves $I(q)$ vs. q for samples with different PVA/CT content obtained using the same FT cycle (a) F12/T12 and (b) F18/T6. For clarity the curves are displaced along the y-axes. Lines are fits to the model of eq. 3 in the main article

Table S1. SAXS parameters obtained from modeling the curves reported in figure S1 with equation 3 of the main article.

Sample	$l_{\text{lor}}(0)$	ζ [nm]	m	$l_{\text{ex}}(0)$	a [nm]
P100%-C0% F6/T18	0.86 ± 0.01	3.8209 ± 0.01	3.37 ± 0.02	101.89 ± 0.84	33.75 ± 0.20
P100%-C0% F12/T12	1.38 ± 0.01	3.84 ± 0.01	3.29 ± 0.02	27.45 ± 0.73	33.41 ± 0.18
P100%-C0% F18/T6	1.05 ± 0.01	3.96 ± 0.01	3.36 ± 0.02	39.76 ± 0.69	25.32 ± 0.17
P85%-C15% F6/T18	1.25 ± 0.01	3.83 ± 0.02	3.36 ± 0.02	139.61 ± 0.97	34.97 ± 0.24
P85%-C15% F12/T12	1.32 ± 0.01	3.77 ± 0.02	3.38 ± 0.02	75.238 ± 0.34	37.93 ± 0.18
P85%-C15% F18/T6	1.30 ± 0.01	3.76 ± 0.02	3.40 ± 0.02	89.038 ± 0.49	30.37 ± 0.18
P70%-C30% F6/T18	2.28 ± 0.01	3.78 ± 0.01	3.50 ± 0.01	168.65 ± 0.32	32.49 ± 0.02
P70%-C30% F12/T12	1.96 ± 0.01	4.01 ± 0.01	3.46 ± 0.01	133 ± 0.22	29.92 ± 0.02
P70%-C30% F18/T6	2.41 ± 0.01	4.03 ± 0.01	3.41 ± 0.01	237.34 ± 0.40	33.88 ± 0.02
P60%-C40% F6/T18	1.04 ± 0.01	3.74 ± 0.02	3.42 ± 0.02	42.06 ± 0.54	24.15 ± 0.12
P60%-C40% F12/T12	1.25 ± 0.01	3.82 ± 0.02	3.41 ± 0.02	52.28 ± 0.69	24.67 ± 0.13
P60%-C40% F18/T6	0.87 ± 0.01	4.12 ± 0.01	3.30 ± 0.02	30.37 ± 0.51	23.21 ± 0.16
P50%-C50% F6/T18	2.09 ± 0.01	3.39 ± 0.01	3.68 ± 0.01	69.92 ± 0.12	23.58 ± 0.01
P50%-C50% F12/T12	1.75 ± 0.01	3.75 ± 0.01	3.48 ± 0.01	105.66 ± 0.21	29.32 ± 0.02
P50%-C50% F18/T6_3	1.77 ± 0.01	3.47 ± 0.01	3.56 ± 0.01	107.87 ± 0.67	28.57 ± 0.12
P30%-C70% F6/T18	1.60 ± 0.01	3.85 ± 0.01	3.52 ± 0.01	44.91 ± 0.08	22.01 ± 0.02
P30%-C70% F12/T12	1.83 ± 0.01	3.99 ± 0.01	3.48 ± 0.01	140.24 ± 0.24	31.71 ± 0.02
P30%-C70% F18/T6	1.34 ± 0.01	3.75 ± 0.01	3.59 ± 0.01	47.79 ± 0.10	23.39 ± 0.02

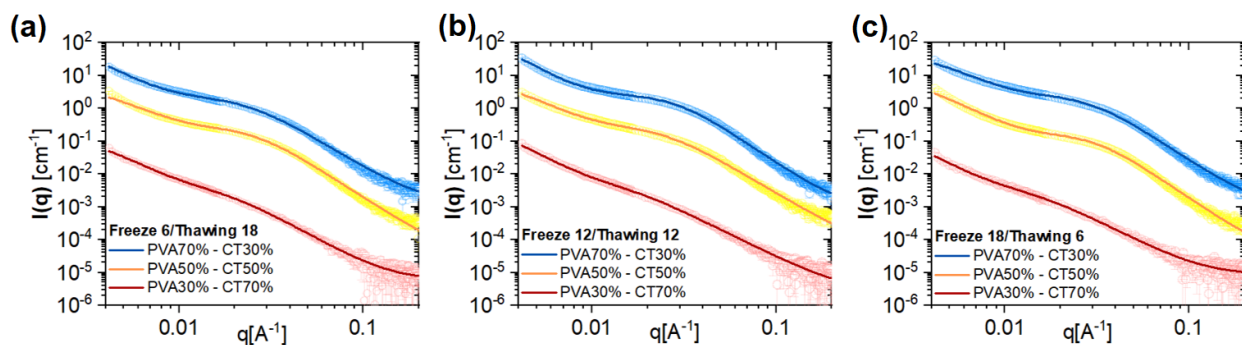


Figure S3. SAXS intensity curves $I(q)$ vs. q for samples with CT Medium- M_w and different PVA/CT, for FT cycles **(a)** F6/T18 and **(b)** F12/T12 and **(c)** F18/T6. For clarity the curves are displaced along the y-axes. Lines are fits to the model of eq. 3 in the main article

Table S2. SAXS parameters obtained from modeling the curves for Medium- M_w of Figure S2 using eq. 3 of the main article.

Sample	$l_{\text{lor}}(0)$	ζ [nm]	m	$l_{\text{ex}}(0)$	a [nm]
P70%-C30% F6/T18	2.12 ± 0.01	4.24 ± 0.01	3.37 ± 0.01	151.61 ± 0.52	34.58 ± 0.04
P70%-C30% F12/T12	2.50 ± 0.01	3.48 ± 0.01	3.76 ± 0.01	488.51 ± 0.91	42.48 ± 0.02
P70%-C30% F18/T6	2.40 ± 0.01	3.39 ± 0.01	3.70 ± 0.01	72.04 ± 0.15	22.39 ± 0.02
P50%-C50% F6/T18	2.49 ± 0.01	3.81 ± 0.01	3.63 ± 0.01	68.86 ± 0.16	22.89 ± 0.02
P50%-C50% F12/T12	2.72 ± 0.01	4.02 ± 0.01	3.34 ± 0.01	109.20 ± 0.23	25.65 ± 0.02
P50%-C50% F18/T6_3	1.57 ± 0.01	3.19 ± 0.01	3.83 ± 0.02	126.93 ± 0.24	26.29 ± 0.02
P30%-C70% F6/T18	0.38 ± 0.01	5.68 ± 0.02	3.12 ± 0.01	23.91 ± 0.13	27.22 ± 0.05
P30%-C70% F12/T12	0.56 ± 0.01	6.54 ± 0.02	2.81 ± 0.01	77.44 ± 0.35	37.16 ± 0.05
P30%-C70% F18/T6	0.37 ± 0.01	6.95 ± 0.02	2.88 ± 0.01	38.03 ± 0.37	38.15 ± 0.11

3. SEM images, confocal stacks and porosity renderings

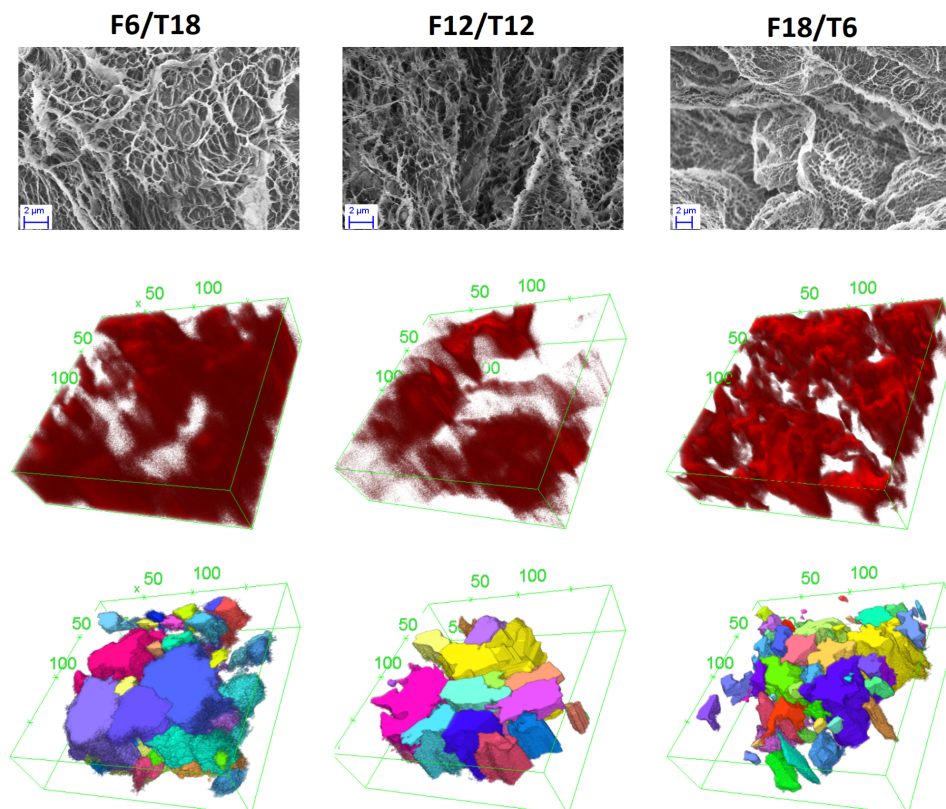


Figure S4. Images correspond to PVA30%- CT70% and different Freeze/Thawing times. **Top** SEM images, scale bar 2 μm. **Middle** 3D confocal microscopy images. **Bottom** Hydrogel pore reconstruction using MorpholibJ, units are in μm.

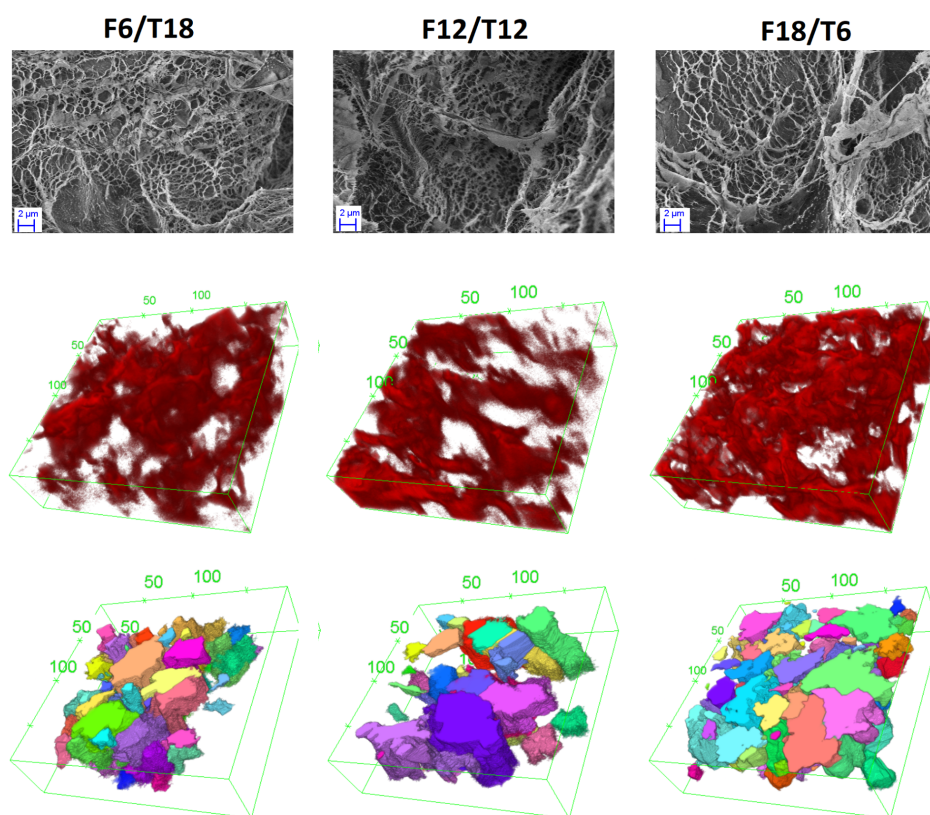


Figure S5. Images correspond to PVA50%- CT50% and different Freeze/Thawing times. **Top** SEM images, scale bar 2 μm. **Middle** 3D confocal microscopy images. **Bottom** Hydrogel pore reconstruction using MorpholibJ, units are in μm.

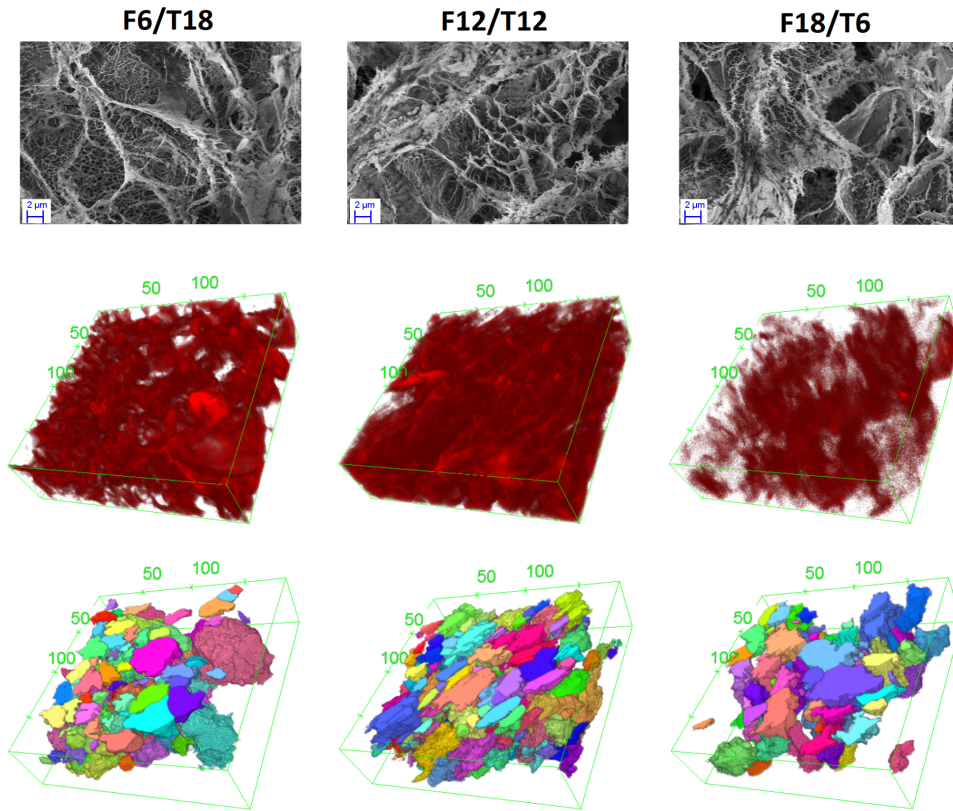


Figure S6. Images correspond to PVA70%- CT30% and different Freeze/Thawing times. **Top** SEM images, scale bar 2 μ m. **Middle** 3D confocal microscopy images. **Bottom** Hydrogel pore reconstruction using MorpholibJ, units are in μ m.

4. 2D porosity parameters and pore volume and sphericity distributions:

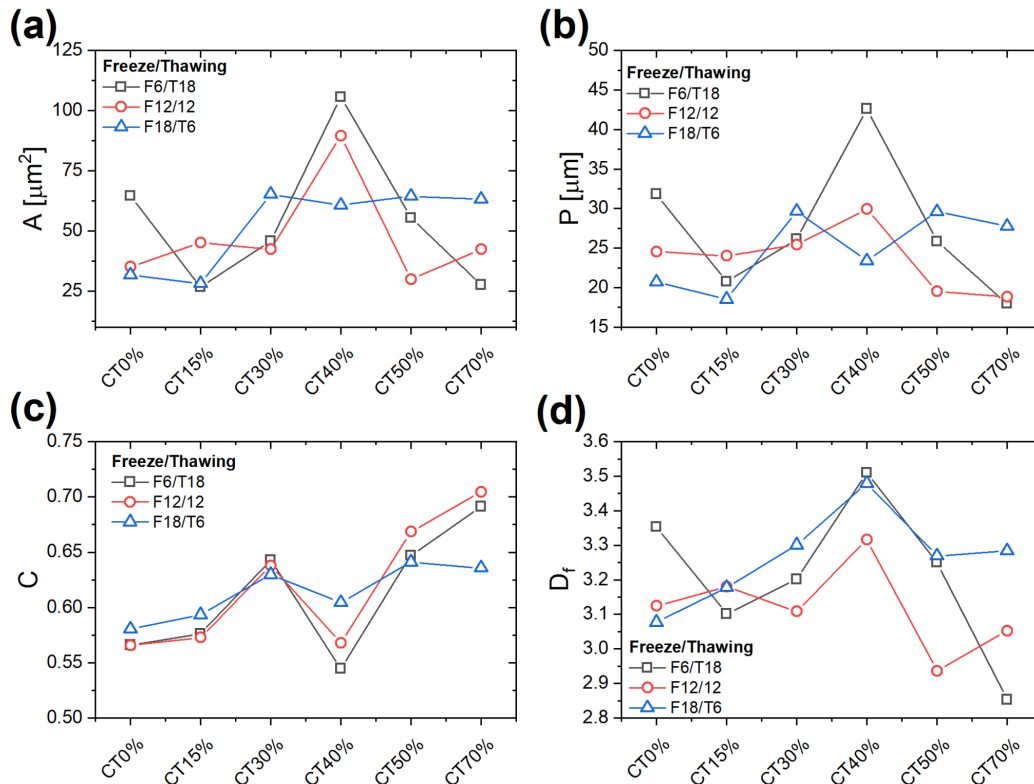


Figure S7. 2D porosity parameters as a function of CT content and for different FT times. **(a)** Average pore area (A) . **(b)** Average pore perimeter (P). **(c)** Circularity (C) parameter calculated as $C = 4\pi(A/P^2)$. **(d)** Fractal dimension of pores D_f , calculated using the relationship; $A \propto P^{2/D_f}$.

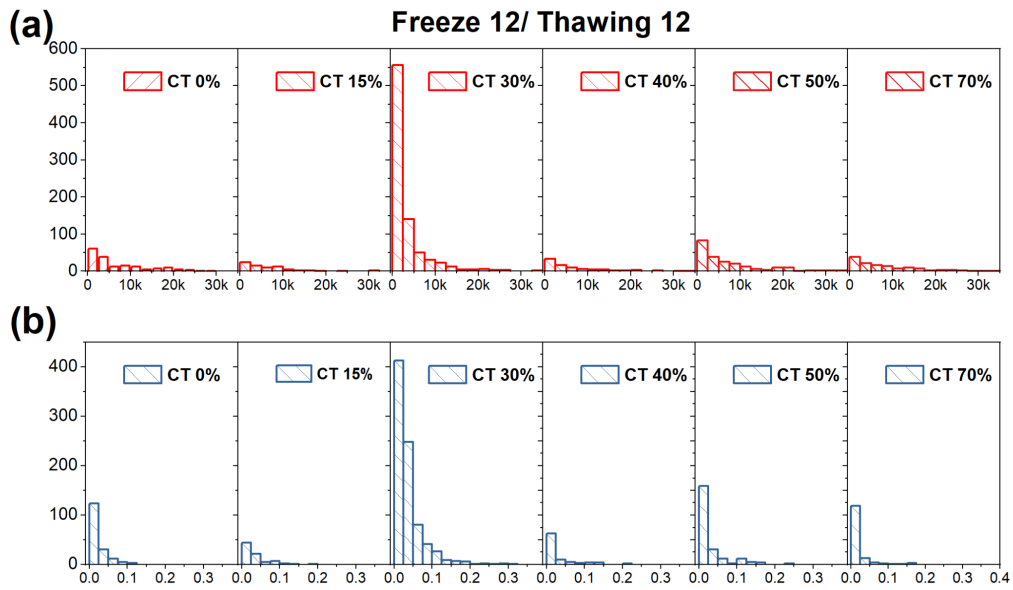


Figure S8. (a) Average pore volume distribution and (b) Sphericity distribution for samples obtained using a F12/T12 cycle and different CT content.

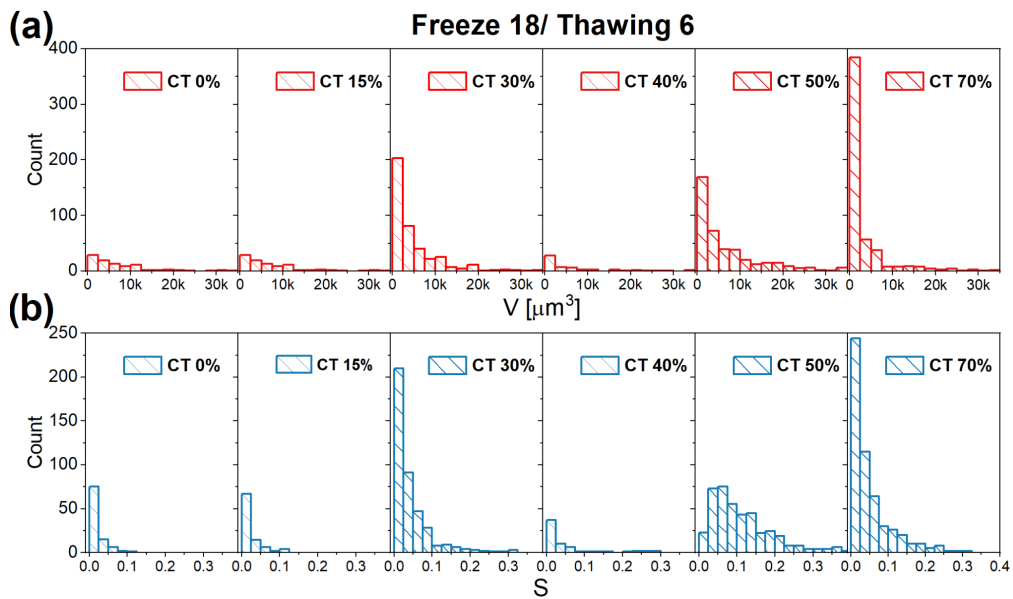


Figure S9. (a) Average pore volume distribution and (b) Sphericity distribution for samples obtained using a F18/T6 cycle and different CT content.

5. Rheological data

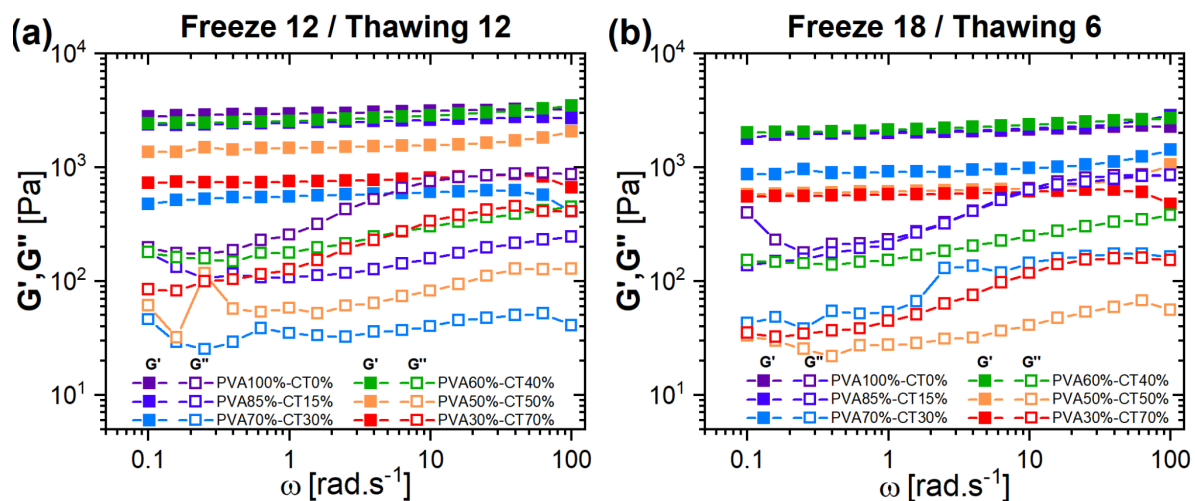


Figure S10. Hydrogel viscoelastic moduli, storage- $G'(\omega)$ and loss- $G''(\omega)$, for different PVA/CT contents and diverse freeze-thawing times **(a)** F12/T12 and **(b)** F18/T6, as a function of oscillation frequency ω .